

Interference effects in a singlet fermion DM model

Jinmian Li

Korea Institute for Advanced Study



December 15th, 2016

Collaboration with P. Ko (arXiv: 1610.03997)

LHC Dark Matter Working Group meeting

- 1 Gauge invariant DM model
- 2 Interference effect of two propagators
 - Cross section
 - Differential distribution
- 3 Interference effect on the CMS search
- 4 Conclusion

Gauge invariant model

Simplest extension of the SM including fermion DM

$$\mathcal{L} = \mathcal{L}_{\text{SM}} + \bar{\chi}(i\not{\partial} - m_\chi - g_\chi S)\chi + \frac{1}{2}\partial_\mu S\partial^\mu S - \frac{1}{2}m_0^2 S^2 \\ - \lambda_{HS}H^\dagger H S^2 - \mu_0^3 S - \mu_1 S H^\dagger H - \frac{\mu_2}{3!}S^3 - \frac{\lambda_S}{4!}S^4$$

After EW symmetry breaking, portal includes two propagators:

$$\begin{pmatrix} h \\ s \end{pmatrix} = \begin{pmatrix} \cos \alpha & \sin \alpha \\ -\sin \alpha & \cos \alpha \end{pmatrix} \begin{pmatrix} H_1 \\ H_2 \end{pmatrix}$$

Interactions of DM and SM particles:

$$\mathcal{L}_{\text{int}} = -(H_1 \cos \alpha + H_2 \sin \alpha) \left[\sum_f \frac{m_f}{v_h} \bar{f}f - \frac{2m_W^2}{v_h} W_\mu^+ W^{-\mu} - \frac{m_Z^2}{v_h} Z_\mu Z^\mu \right] \\ + g_\chi (H_1 \sin \alpha - H_2 \cos \alpha) \bar{\chi}\chi$$

Gauge invariant model

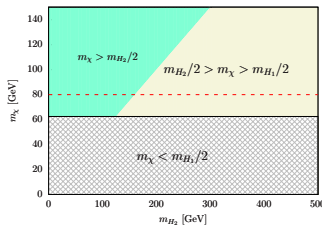
Consequences of gauge symmetry: Interference effect of two propagators

- DM direct detection blind window at $m_{H_1} \sim m_{H_2}$.

S. Baek, P. Ko, W. Park, arXiv:1112.1847

- Collider phenomenology.

S. Baek, et.al, arXiv:1506.06556; P. Ko, H. Yokoya, arXiv:1603.04737

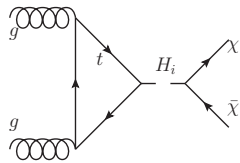


$$m_{H_1} = 125 \text{ GeV}, \quad \sin \alpha = 0.2,$$
$$g_\chi = 1, \quad m_\chi = 80 \text{ GeV},$$
$$m_{H_2}, \Gamma_{H_2}$$

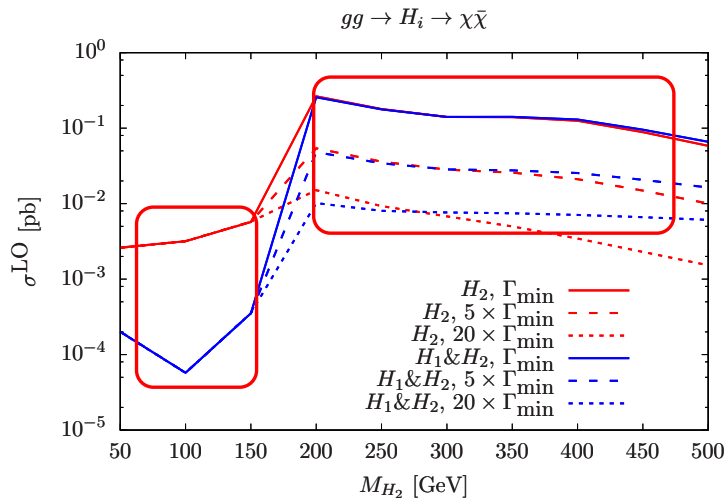
- H_1 is identified as the 125 GeV SM Higgs, decay width $\cos^2 \alpha \cdot \Gamma_{h_{\text{SM}}}$.
- Fix $\sin \alpha = 0.2$ and $g_\chi = 1$, cross sections proportional to $g_\chi \sin 2\alpha$ when Γ_{H_i} are small.
- $m_\chi > m_{H_1}/2$ to avoid SM Higgs invisible decay, but not too heavy so its production cross section can be large.

Total cross section

Taking the gluon-gluon fusion process as an example



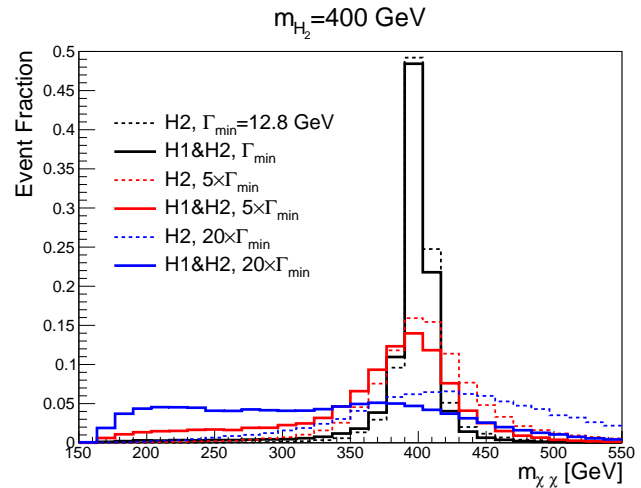
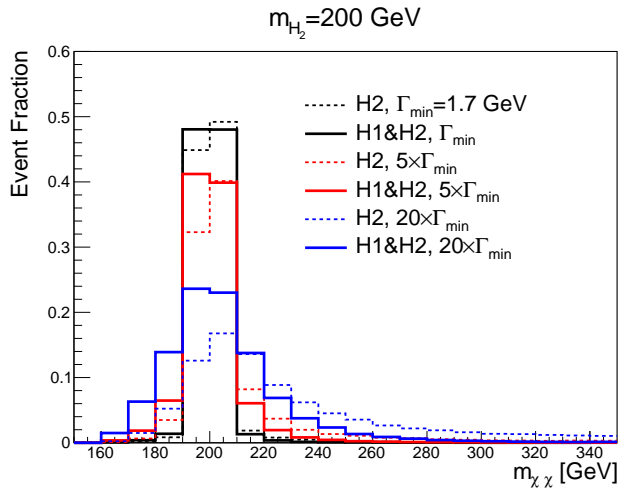
$$\frac{d\sigma_i}{dm_{\chi\bar{\chi}}} \propto \left| \frac{\sin 2\alpha g_\chi}{m_{\chi\chi}^2 - m_{H_1}^2 + im_{H_1}\Gamma_{H_1}} - \frac{\sin 2\alpha g_\chi}{m_{\chi\chi}^2 - m_{H_2}^2 + im_{H_2}\Gamma_{H_2}} \right|^2$$



- Γ_{\min} for H_2 is calculated by assuming H_2 decays only into SM particles and DM pair, $\sin \alpha = 0.2$ and $g_\chi = 1$.
- H_2 scenario corresponds to the usual singlet scalar portal DM model.
- Including H_1 will substantially reduce the DM pair production cross section when $m_{H_2} \lesssim 2m_\chi$.
- $H_1 \& H_2$ scenario has smaller cross section than the usual H_2 scenario when $m_{H_2} \in (2m_{\chi\chi}, \sim 270 \text{ GeV})$ and larger cross section when $m_{H_2} \gtrsim 270 \text{ GeV}$

Differential distribution on $m_{\chi\chi}$

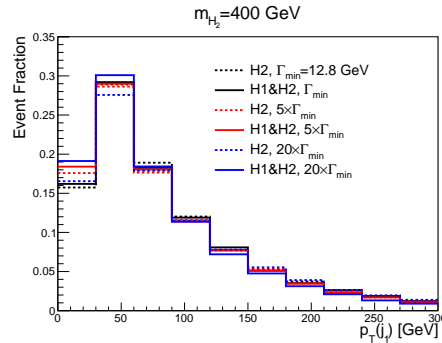
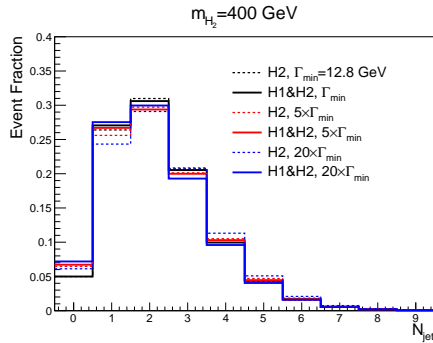
$$\frac{d\sigma_i}{dm_{\chi\chi}} \propto \left| \frac{\sin 2\alpha g_\chi}{m_{\chi\chi}^2 - m_{H_1}^2 + im_{H_1}\Gamma_{H_1}} - \frac{\sin 2\alpha g_\chi}{m_{\chi\chi}^2 - m_{H_2}^2 + im_{H_2}\Gamma_{H_2}} \right|^2$$



- Enhancement in event fraction for $m_{\chi\chi} \in (2m_\chi, m_{H_2})$ and deduction in event fraction when $m_{\chi\chi} > m_{H_2}$.
- For $m_{H_2} = 200 \text{ GeV}$, the total event fraction in $(2m_\chi, m_{H_2})$ is smaller than that in $(m_{H_2}, +\infty)$ while it is opposite for $m_{H_2} = 400 \text{ GeV}$. Leading to reduced total cross section for $m_{H_2} = 200 \text{ GeV}$ and increased total cross section for $m_{H_2} = 400 \text{ GeV}$.

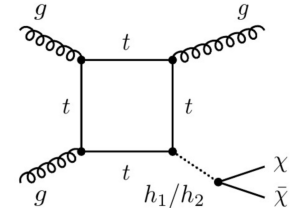
Shape of collider observables

- $m_{\chi\chi}$ is not a physical observable at hadron colliders.
- The QCD radiation is proportional to the $m_{\chi\chi}$.



- The interference effect increases the event rate in low $m_{\chi\chi}$ region and reduces the event rate in high $m_{\chi\chi}$ region.
- The $H_1&H_2$ scenarios has lower jet multiplicity and softer $p_T(j_1)$ distribution comparing to the usual H_2 scenarios.
- The differences become larger for a wider H_2 decay width.

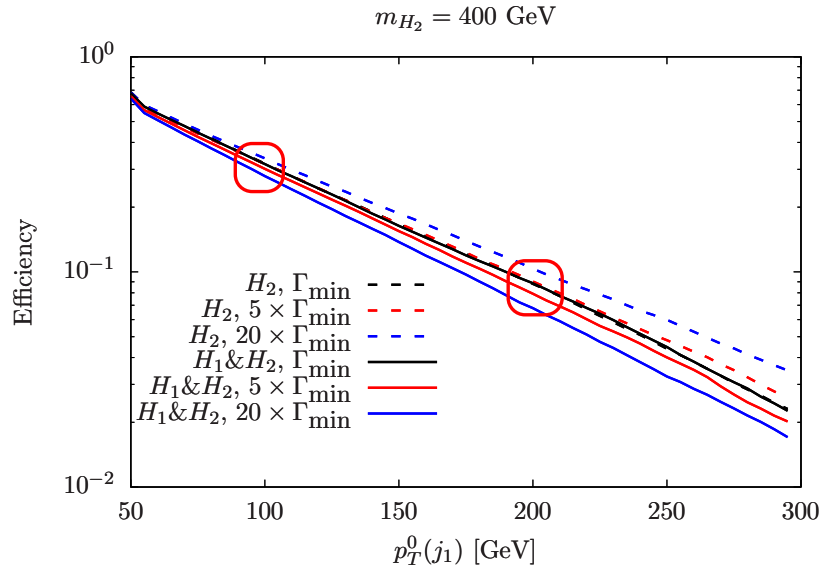
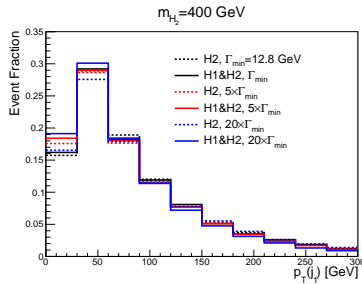
- Benchmark point $m_{H_2} = 400$ GeV.
- GGF production with addition jet from ISR or from top loop.



- Parton showering with Pythia.

Cut efficiency (cumulative curve)

Cut efficiency of $p_T(j_1) > p_T^0(j_1)$:

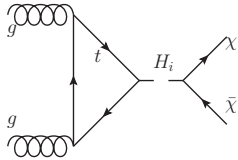


- The difference in efficiencies between $H_1 \& H_2$ and H_2 scenarios becomes more significant for more stringent $p_T(j_1)$ cut and/or larger H_2 decay width
- $\Gamma(H_2) = 20 \times \Gamma_{\min}$, the efficiency ratios (defined as $\frac{\epsilon(H_1 \& H_2)}{\epsilon(H_2)}$) are 0.83 and 0.66 for $p_T(j_1) > 100$ GeV and $p_T(j_1) > 200$ GeV cuts, respectively
- $\Gamma(H_2) = 5 \times \Gamma_{\min}$ the corresponding efficiency ratios are 0.95 and 0.88.

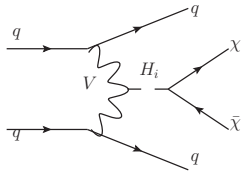
- Mono-jet cuts: (1). Events are required to have missing transverse momentum $p_T^{\text{miss}} > 200$ GeV. (2). A event is vetoed if it contains any isolated leptons, isolated photon, τ -tagged jets and b-tagged jets. (3). The jets are clustered using anti- k_t algorithm with $R = 0.4$ (denoted by j^{ak4}). The leading j^{ak4} is required to have $p_T(j_1^{\text{ak4}}) > 100$ GeV and $|\eta(j_1^{\text{ak4}})| < 2.5$. (4). The minimum azimuthal angle between the \vec{p}_T^{miss} and leading four j^{ak4} s with $p_T > 30$ GeV is required to be greater than 0.5.
- Mono-V cuts: (1). A more stringent cut on p_T^{miss} is applied, $p_T^{\text{miss}} > 250$ GeV. (2). The final states particles are reclustered using anti- k_t algorithm with $R = 0.8$, denoted by j^{ak8} . The leading j^{ak8} should has $p_T(j_1^{\text{ak8}}) > 250$ GeV and $|\eta(j_1^{\text{ak8}})| < 2.4$. (3). Invariant mass of the leading j^{ak8} after pruning is required to be between 65 and 105 GeV. (4). The N-subjettiness variable τ_N is used to discriminate the two prong decays of the vector boson from QCD jets. The leading j^{ak8} is required to have $\tau_2/\tau_1 < 0.6$.

Events that pass both mono-jet cuts and mono-V cuts are assigned to the mono-V SR. And those that pass the mono-jet cuts while fails any of these mono-V cuts are assigned to the mono-jet SR. $N_{\text{mono-jet/mono-V}}^{\text{upper}} = 11000/450$.

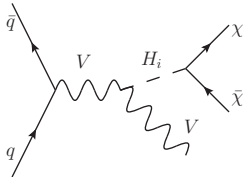
DM production processes



Additional jet radiated either from initial state or from top loop; jet is required to have $p_T > 100$ GeV; NNLO K-factor ~ 2.5

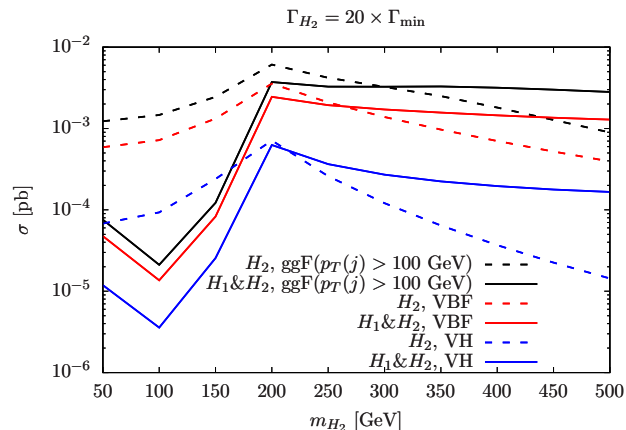
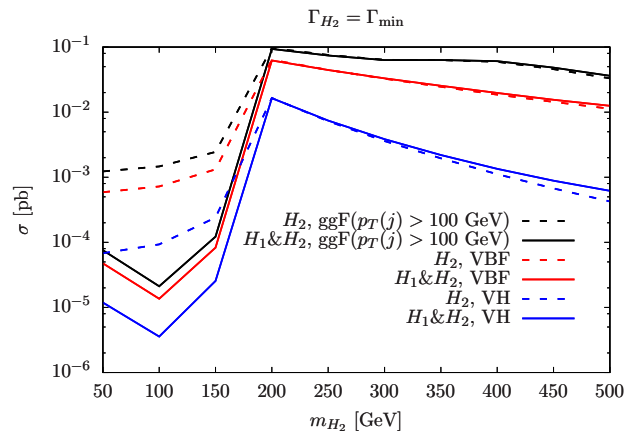


Two forward-backward jets at LO; jets are required to have $p_T > 20$ GeV



V includes W^\pm/Z ; boosted V decaying hadronically can form the V -jet; NLO cross section calculated by MG5

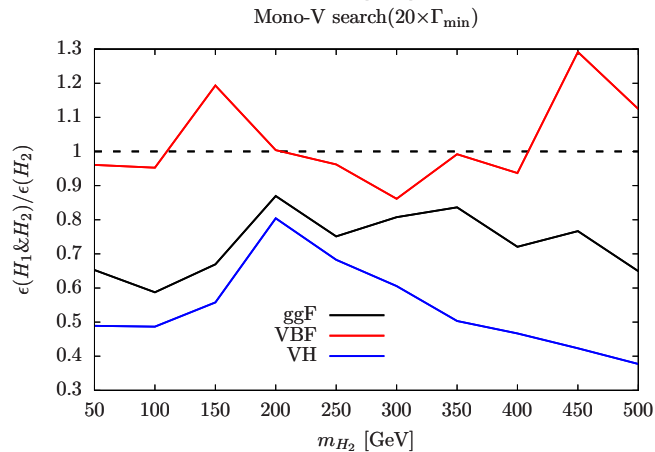
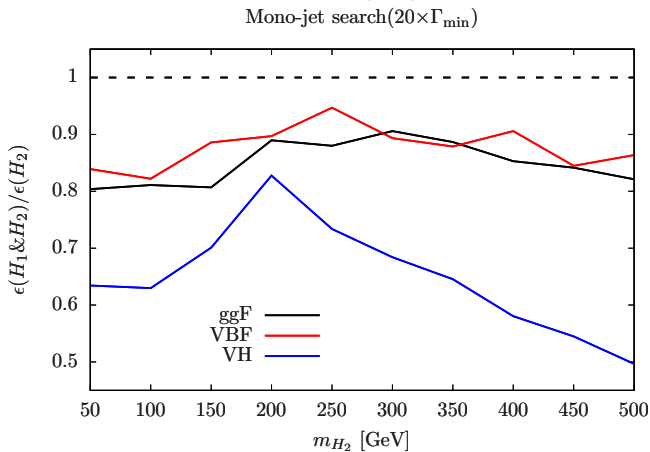
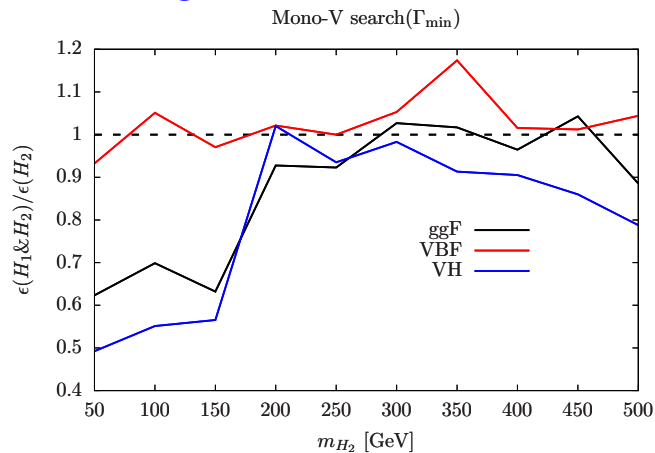
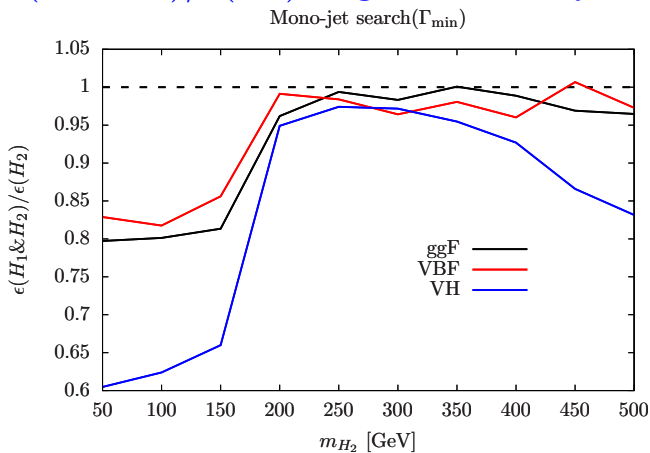
DM production cross sections



- The main features of this figure regarding the variations of m_{H_2} and $\Gamma(H_2)$ follows the general arguments as before.
- GGF is the most dominant production process even after the stringent cut on the radiated jet, VH is around one to two orders of magnitude smaller.
- The interference effect between two propagators is most significant in VH process.

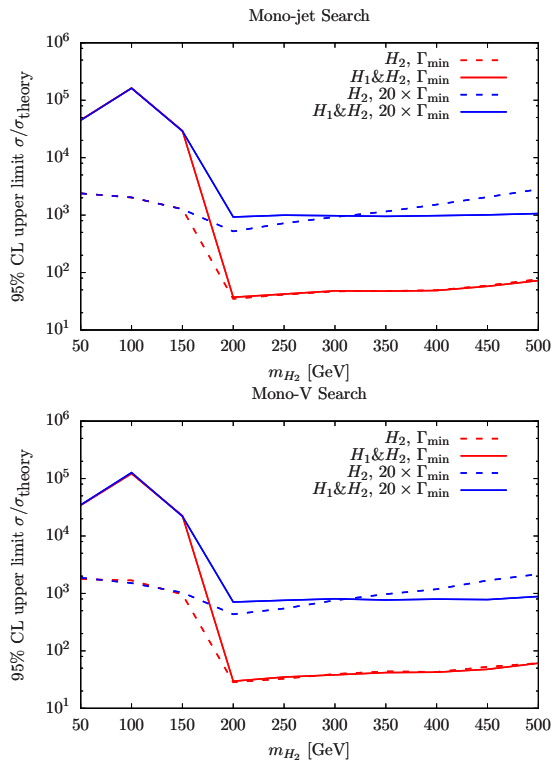
Signal efficiency in the CMS search

$\epsilon(H_1 \& H_2)/\epsilon(H_2)$: signal efficiency ratios between signals with and without H_1 .



Bounds from the CMS search

$$\mu_{\text{mono-jet/mono-V}}^{\text{limit}} = \frac{\sigma}{\sigma_{\text{theory}}} = \frac{N_{\text{mono-jet/mono-V}}^{\text{upper}}}{\sum_{i=\text{ggF, VBF, VH}} \mathcal{L} \times \sigma_i \times \epsilon_i^{\text{mono-jet/mono-V}}}$$



Features of the exclusion bounds are approximately described by the inverse of the production cross sections.

- In $m_{H_2} < 2m_\chi$, the reduction of cross section due to destructive interference and off-shell effect leads to very weak bound in the $H_1 \& H_2$ scenario.
- The interference effect on cross section leads to smaller cross section when $m_{H_2} \in (2m_{\chi\chi}, 270 \text{ GeV})$ and larger cross section when $m_{H_2} > 270 \text{ GeV}$.
- The reduction of signal efficiency from interference effect will enlarge the difference in search sensitivities for $m_{H_2} \in (2m_{\chi\chi}, 270 \text{ GeV})$ and shrink it for $m_{H_2} > 270 \text{ GeV}$.
- Signal cross section in our model is at least one order of magnitude below the current reach.
- The mono-V search has slightly better sensitivity than the mono-jet search.

Signal composition

Benchmark point $m_{H_2} = 400$ GeV	Mono-jet SR			Mono-V SR		
	ggF	VBF	VH	ggF	VBF	VH
H_2, Γ_{\min}	194.4	22.3	2.9	7.8	1.2	1.4
$H_1 \& H_2, \Gamma_{\min}$	197.0	22.7	3.2	7.7	1.3	1.5
$H_2, 20 \times \Gamma_{\min}$	6.2	0.82	0.092	0.28	0.049	0.043
$H_1 \& H_2, 20 \times \Gamma_{\min}$	9.2	1.5	0.28	0.36	0.094	0.11

- The ggF is always the most dominant process.
- The VH becomes is important in the mono-V search, in spite of its small production cross section.
- The interference effect tends to increase the composition of VH in both SRs, especially for the scenario with large H_2 decay width.

- Simplified model with gauge symmetry includes two propagators, which will interfere with each other thus changing the DM and SM interactions.
- At LHC, this interference effect can be either constructive or destructive in the DM production cross section depending on both singlet scalar and DM masses, and it will soften the final state jets in the full mass region.
- The interference effect plays a very important role in the DM search sensitivity.